Au-segregated dealloying and Pd-induced clock reconstructing of Cu(001)

1996 J. Phys.: Condens. Matter 8 4903

(http://iopscience.iop.org/0953-8984/8/27/004)

J. Phys.: Condens. Matter **8** (1996) 4903–4918. Printed in the UK

Au-segregated dealloying and Pd-induced clock reconstructing of Cu(001)

Y G Shen†, J Yao, D J O'Connor, B V King and R J MacDonald
Department of Physics, University of Newcastle, New South Wales 2308, Australia

Received 12 January 1996, in final form 26 March 1996

Abstract. The structure and growth of ultrathin Au and Pd films on Cu(001) have been studied by low-energy ion scattering (LEIS) and low-energy electron diffraction (LEED). Due to the existence of a kinetic pathway for intermixing, both Au and Pd are incorporated into the Cu(001) surface at room temperature, forming a c(2 × 2) surface alloy at a coverage of 0.5 monolayer (ML). At Au coverage near 1.2 ML, the surface layer is pure Au; this is caused by Au-induced segregation from the underlying c(2 × 2) layer to the surface. No second- and/or third-layer Au is evident. In contrast to this, for the Pd/Cu(001) case a (2 × 2)p4g clock reconstruction is formed after deposition of 1 ML Pd. The LEIS data, through comparisons with 3-D computer simulation, reveal a 0.25 Å lateral clockwise–anticlockwise displacement of the first-layer Pd atoms. A simple model for this clock reconstruction is proposed. The driving force behind the dealloying for the Cu–Au alloy and Pd-induced reconstructing for the Cu–Pd surface is also discussed.

1. Introduction

Intermixing, alloying, dealloying and strain-induced reconstructing at surfaces are important concerns in the growth of thin films on metal substrates. Many studies show that these processes may strongly influence the electronic structure, and change many physical and chemical properties of film surfaces. In recent years, the interaction of Au and Pd with the Cu(001) surface has been extensively studied experimentally and theoretically [1–15]. Interest in these systems has been motivated by the fact that Cu-based bimetallic catalysts show very useful properties, particularly in respect of their industrial applications, such as materials selectivity, structural stability and catalytic activity in comparison to their single-metal counterparts. These properties can be controlled by tailoring the local composition of the bimetallic surface.

For both Au and Pd deposition on Cu(001), intermixing at RT (room temperature) plays a significant role. In one of the earliest studies of these systems [1], a c(2 × 2) structure from visual inspection of the LEED pattern at Au coverage of $\Theta_{Au} = 0.5$ ML on Cu(001) indicated the formation of an ordered Cu_3Au-like surface alloy. The formation of a mixed ordered Cu–Au layer has been confirmed using LEED I–V analysis and photoelectron diffraction [2, 3]. While the evidence for alloy formation is strong, the experimental results concerning how the alloy monolayer forms are still puzzling: several recent studies show that deposition of additional Au on the c(2 × 2) surface at RT leads to a segregation of the Au from the underlying c(2 × 2) layer to the surface, effectively dealloying the subsurface

† Corresponding author. Fax: +61 49 216907; e-mail: phsy@cc.newcastle.edu.au.

0953-8984/96/274903+16$19.50

[4–6]. However, other studies indicate that the local formation of a Cu_3Au-like surface alloy extends over at least three layers even at 1 ML [7, 8].

For Pd deposition on Cu(001) at RT, the conclusion of the formation of an ordered c(2 × 2) surface alloy formed at 0.5 ML Pd remains unchallenged [9–12]. Somewhat surprisingly, at ML coverage several groups have reported different observations although the same preparation technique was used. While most of the studies find the weak (1 × 1) pattern, Pope *et al* [13, 14] report a p(2 × 2) structure. A very recent study also by Pope *et al* [15] has confirmed that this last structure is in fact a (2 × 2)p4g phase. The clock reconstruction formed at 1 ML coverage is due to domains of 80% pure Pd islands with the p4g symmetry mixed with a 20% c(2 × 2) region above a mixed c(2 × 2) layer [15]. However, this model is obviously contradictory to a local coverage of the surface. In addition, it is far from clear how the metal-induced reconstruction of fcc(001) is derived by the interaction between surface layers.

In this work, the first LEIS results for the Au/Cu(001) and Pd/Cu(001) systems are presented, in which new features not reported in the earlier studies of these systems have been revealed. LEIS is well established as a probe for both surface composition and surface structure. It is well known that LEIS using noble-gas ions (such as He^+) is a highly surface-sensitive technique for investigating surface structure due to the high neutralization rate of noble-gas ions scattering from below a surface. However, analysis of low-energy noble-gas-ion scattering has been hindered by a trajectory-dependent neutralization probability (i.e. a drastic reduction of the measured focusing effects) (see a recent review [16]). The understanding of the neutralization process of noble-gas ions is far from complete, so the analysis of experimental results has often been difficult. For this reason, the use of alkali ions (such as Li^+) instead of noble-gas ions to probe surface structure in LEIS has become more common because of their low neutralization probability and trajectory independence [16]. Over the past fifteen years, work on alkali-ion beams, time-of-flight (TOF) scattering techniques, computer simulation and numerous structural determinations have established LEIS as a modern surface analysis technique [16–18]. This technique is therefore especially suited to investigating the initial stage of growth and structure of the surface alloys.

The measurements unambiguously show that for Au deposition on Cu(001), an ordered c(2 × 2) surface alloy at 0.5 ML and a pure hexagonal close-packed (hcp) Au overlayer at 1.2 ML are formed. Since no second- or third-layer Au was observed at 1.2 ML, the formation of the Au (1 × 1) overlayer is due to dealloying caused by the additional deposited Au between 0.6 and 1.2 ML. For the case of Pd on Cu(001), the LEIS data indicate that the observed p4g structure at 1 ML Pd consists of the two mixed surface layers: a randomly intermixed Cu–Pd region with some Pd islands (20%) in the top layer, and an ordered c(2 × 2) region in the second layer. From the LEIS data and 3-D computer simulation, the lateral displacement of the surface Pd atoms is determined to be 0.25 ± 0.07 Å. Finally, a novel driving force for this clock reconstruction is discussed in terms of the intuitive hard-sphere model of atomic stacking.

2. Experimental procedure

Our angle-resolved ion-scattering system has been described elsewhere [19, 20]. Briefly, the UHV chamber ($\sim 1 \times 10^{-10}$ mbar base pressure) was equipped with a three-grid LEED optics. The angle of incidence, α, measured from the surface plane, was calibrated by aligning a He–Ne laser along the ion beam direction. The azimuthal angle, ϕ, was measured from the [110] azimuth of clean Cu(001). The angle was initially determined by LEED measurements and then more finely adjusted using azimuthal scans in LEIS. The scattered

ions were energetically analysed by a hemispherical electrostatic analyser ($\Delta E/E = 0.02$), which is rotatable to allow variation of the total laboratory scattering angle θ from 0 to 130°. The accuracies of the angles α, ϕ and θ were $\pm 0.5°$, 1° and 1° respectively. The analyser was equipped with a dual multichannel detector (MCD) to provide high count rates. The use of MCD allows data collection with small ion doses to avoid any significant damage or desorption during the measurements.

Both Au and Cu were deposited by evaporation from resistively heated tungsten baskets. Pressures during evaporation were 3×10^{-10} mbar for Au and 4×10^{-10} mbar for Pd. Most Au and Pd depositions were done onto RT substrates, but in some cases Au was deposited onto a cooled or heated sample as described in the text. The Au coverages for the nominal 0.5 and 1.0 ML samples used for LEIS measurements were determined as follows: due to the presence of two sharp LEED patterns within the first monolayer, a c(2×2) phase at 0.5 ML at RT and a c(14×2) phase at 1 ML at -50 °C. The Pd coverage was estimated from the evaporation time, and the assumptions that the best c(2×2) phase is 0.5 ML and the optimum p4g structure is 1 ML. Excellent reproducibility of the evaporation rate was achieved by using an evaporator power supply that regulated the emission current. The evaporation rate was estimated to be accurate to $\pm 15\%$ for Au and $\pm 10\%$ for Pd.

The well oriented ($\leqslant 0.5°$) and polished Cu(001) sample was cleaned by repeated cycles of Ar^+-ion bombardment and annealing at 600–650 °C. Surface cleanliness was verified by the absence of O, S and C in the He^+ LEIS spectra.

3. Results

3.1. Au/Cu(001)

Figure 1 shows the results of the azimuthal ϕ-scans, collected from clean, 0.5 ML, 1 ML and 5 ML Au-covered Cu(001) surfaces at grazing incidence. For the clean Cu(001) surface, pronounced deep minima are observed at the ϕ-positions corresponding to alignment of the beam along specific directions because the scattering centres are inside of the shadow cones cast by the aligned nearest neighbours. As ϕ is scanned, the scattering centres move out of the shadow cones along intermediate ϕ-directions where atoms are not aligned, and a resulting increase in intensity is observed [16–20]. The largest shadow cone centred around the [110] azimuth indicates the closest separation in this direction. The fact that the shadowing dips of the Cu and Au signals obtained from the c(2×2) surface are centred at $\phi = 0$ and 45° corresponding to rows of the Cu and Au atoms aligned in these directions confirms that the Au atoms are incorporated into the first layer by the substitution for Cu with Au atoms. For the 1 ML case, the Cu intensity is reduced to about 10–15% of the clean surface intensity, indicative of a nearly pure Au layer formed on the surface. The appearance of several shadowing dips at around $\phi = -15$, 15 and 45° in the Au scan reveals the symmetry of a hcp(111) Au overlayer. The fact that the shadowing dip at $\phi = 15°$ is more pronounced compared to those at $\phi = -15$ and 45° could be interpreted as the predominance of one domain in the surface layer. It therefore appears that the surface layer has indeed transformed into a hcp arrangement. This is in close resemblance to the ratio of the atomic densities of the (001) and (111) planes (0.87). The result is also supported by the LEED observations, which show a change from a c(2×2) to a pattern with both hcp spots as well as the fourfold pattern of Cu(001) (see the photographs of LEED patterns on the right-hand side of the figure).

We conclude that the formation of a near-pure Au overlayer is due to dealloying caused by the additional deposited Au, in agreement with previous studies [4, 5]. At $\Theta_{Au} = 5$ ML,

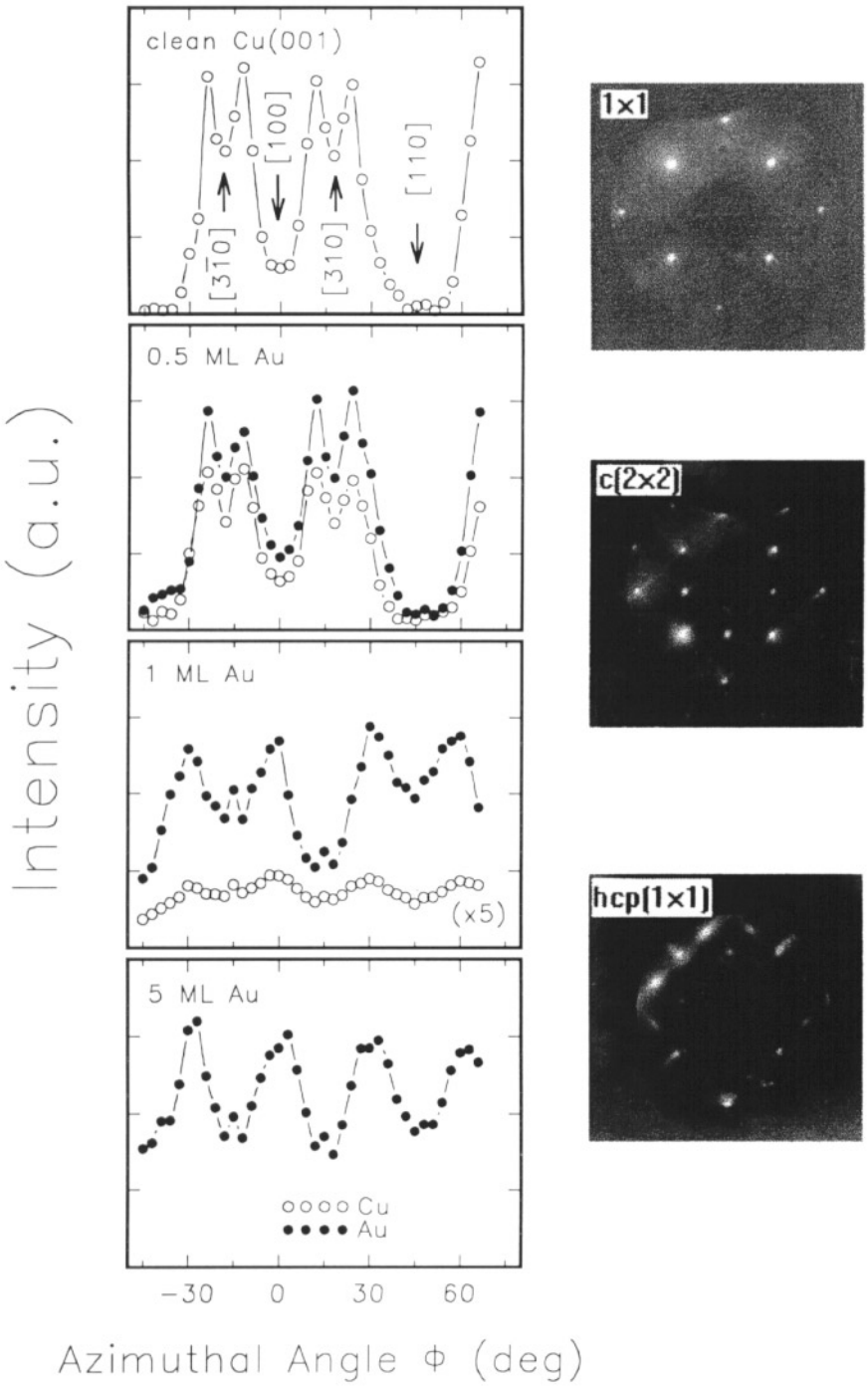

Figure 1. Azimuthal distributions of 1 keV Li^+ ions from clean and well annealed Cu(001), and 0.5 ML, 1 ML and 5 ML Au-covered Cu(001) surfaces at an incident angle of $\alpha = 10^\circ$ and a fixed scattering angle of $\theta = 110^\circ$. Photographs of LEED patterns for Cu(001) (80 eV), c(2 × 2) (0.5 ML, 124 eV) and hcp (1 × 1) (1 ML, 74 eV) are also shown on the right-hand side of the figure.

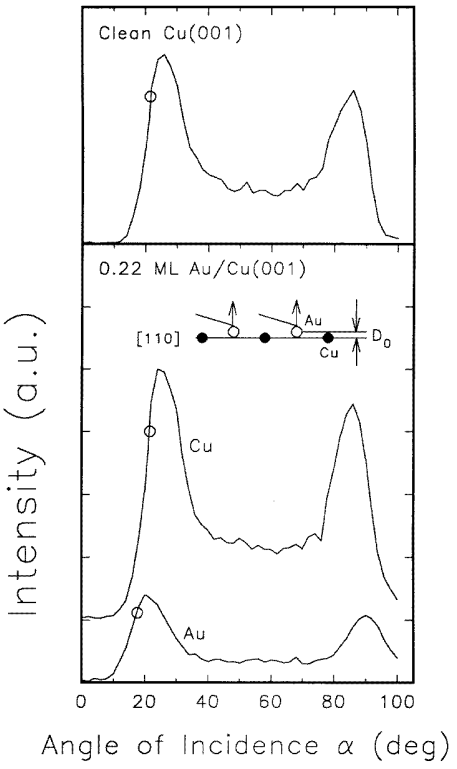

Figure 2. Intensities of 1 keV Li^+ ions scattered from the clean Cu(001) and 0.22 ML Au/Cu(001) surfaces. The incidence angle scans were performed along the [110] azimuth at $\theta = 110^\circ$ by varying the incidence angle between the beam and surface from 0 (i.e. the beam parallel to the target surface) to 100° in 2° intervals. The critical angles α_c are indicated by open circles.

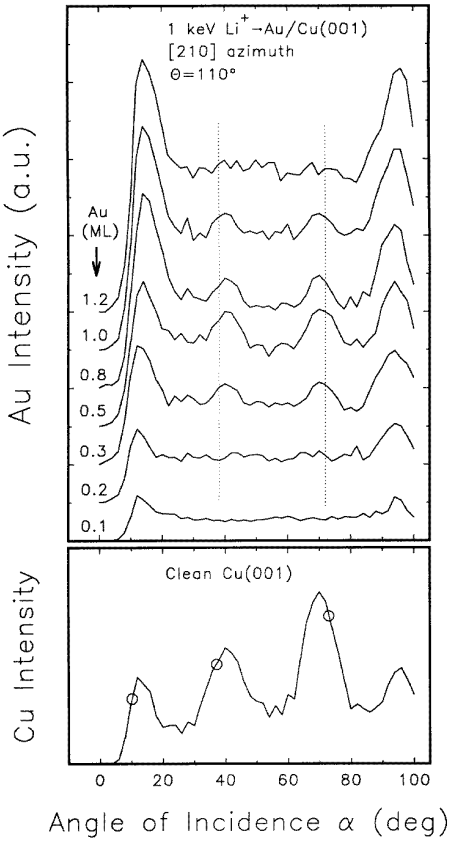

Figure 3. Incidence angle (α-) scans (in 2° intervals) along the [210] azimuth at $\theta = 110^\circ$ for various Θ_{Au} on Cu(001).

the formation of a Au(111) film is observed. At this stage, the Au ϕ-scan shows typical shadowing features of the fcc(111) surface [20], which has two equivalent domains. This is also consistent with our observations of a hcp LEED pattern with 12 elongated spots.

To properly characterize the surface structure it is important to test whether there is any buckling of the mixed Cu–Au layer. The existence of a surface-buckling effect should be most readily visible in the incidence angle α-scan on setting the scattering plane along a row (the shortest azimuth) containing both Au and Cu atoms. This has been done by collecting the data in the α-scans along the [110] azimuth, and typical experimental data from a clean surface and from the Cu–Au surface (0.22 ML Au) are shown in figure 2, where the peak-area intensities of the Cu and Au are plotted as functions of α. For each scan the ion intensity at small α-values is low because each surface atom lies in the shadow cone cast by its preceding neighbour. On increasing α, the atoms of the first layer (also possible for the second layer if it is directly exposed to the beam) move out of the shadow

cone at a critical angle α_c. The sharp rises with a well defined maximum observed in the α-scan of figure 2 are due to focusing of the ion trajectories at the edge of the cone. We determined the position of the critical angle α_c (the shadowing edge) corresponding to 80% of the maximum intensity [19].

At low coverage, no diffusion of Au atoms into the Cu substrate was observed below 0.25 ML (for evidence see below). Furthermore, no Au islands were observed at the Cu–Au surface for $\Theta_{Au} \leqslant 0.5$ ML [2, 3]. Therefore, the shadowing edge at $\alpha_c = 17.6^\circ$ in the Au scan is due to shadowing of first-layer Au atoms by neighbouring Cu atoms at angles below the critical angle as illustrated by the inset diagram in figure 2, while the shadowing edge at $\alpha_c = 21.5^\circ$ in the Cu scan is contributed by both the first-layer Au shadowing of first-layer Cu and second-layer Cu shadowing of second-layer Cu because the second-layer Cu atoms are directly exposed to the beam along this azimuth. Although Au atoms are incorporated into the first Cu layer, the fact that the shadowing edge is shifted to a lower angle by $\sim 4^\circ$ in the Au scan compared to that in the Cu scan indicates that the Au atoms are not coplanar with neighbouring Cu atoms in the top layer.

To determine the relative positioning of the Cu and Au atoms from the value of the critical angle α_c along the [110] azimuth, providing a measure of any surface buckling, D_0, it is first necessary to calibrate the scattering potential for the interaction of Li^+ ions and surface Cu and Au atoms. Using a Thomas–Fermi–Molière (TFM) potential with screening lengths of 0.78 a_F and 0.90 a_F for Li^+ scattered from Cu and Au atoms respectively [21], a value of $D_0 = 0.12 \pm 0.06$ Å is determined, in good agreement with the literature values of 0.1 Å [2] and 0.18 Å [8]. This height is based upon the measurements made at four different scattering angles between 90 and 120°. Details on the method and on its previous applications to different systems can be found in [20]. Analysis using the Ziegler–Biersack–Littmark (ZBL) potential yields a value of 0.15 ± 0.06 Å, roughly indicating an uncertainty due to using a different scattering potential.

To further clarify the dealloying effect caused by additional Au deposition onto the c(2 × 2) alloy, α-scans along the [210] azimuth have been performed. Figure 3 shows the Au intensities obtained from the α-scans along the [210] azimuth, collected as a function of Au coverage at $\theta = 110^\circ$. The α-scan from the clean Cu(001) surface under the same scattering geometrical conditions is also shown in figure 3 for reference. For the clean Cu(001) surface, the intensity of the single-scattering shadowing edge at $\alpha_c = 9.8^\circ$ results from first-layer Cu atoms. The second shadowing edge at $\alpha_c = 38.5^\circ$ is attributed to first-layer Cu atoms focusing onto second-layer Cu atoms. Simultaneously Li^+ ions are focused from second-layer Cu atoms onto third-layer Cu atoms.

The blocking edge observed at $\alpha_b = 72.5^\circ$ arises because the outgoing Li^+ ion scattered by the second- (also third-) layer Cu atom passes near a blocking atom in the first (also second) layer. At the initial stage of Au deposition ($\leqslant$0.2 ML), the fact that there is only one shadowing edge at around $\alpha_c = 10^\circ$ and the flat angular dependence above 18° in the Au scan indicate that Au is only in the topmost layer. If there were substrate (second- or third-layer) Au atoms, we would have seen additional shadowing features at high incidence angles. On increasing Θ_{Au} to 0.3 ML, a new shadowing edge at around $\alpha_c = 38^\circ$ as well as a new blocking edge at about $\alpha_b = 72^\circ$ are observed, indicating that there is substrate Au. At 0.5 ML, the second shadowing peak (also the blocking peak) becomes more pronounced. Taking the scattering cross section into account, we estimate that approximately 15% of deposited Au atoms are located in the second and/or third layers. Our composition measurements support this estimation.

We conclude that, during the c(2 × 2) surface alloy formation, a certain amount of Au atoms may be buried in the second or third layer, even if the Au segregation towards the

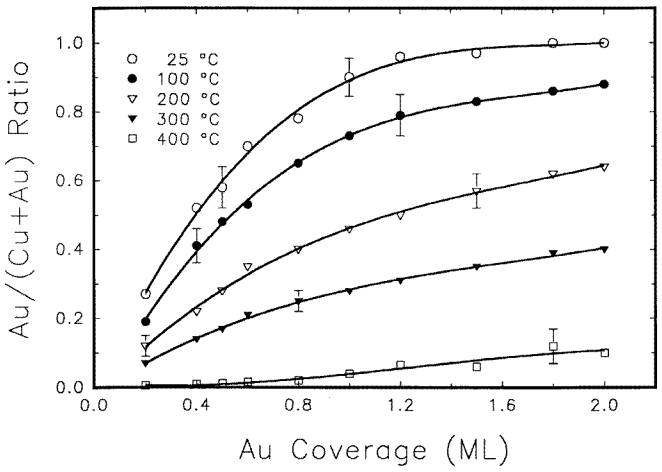

Figure 4. The normalized top-layer Au/(Au + Cu) intensity ratio as a function of Θ_{Au} with 1 keV Li^+ ions under double-alignment conditions ([100] azimuth, $\theta = 2\alpha = 90°$) at five different substrate deposition temperatures.

surface is energetically favoured. Further deposition of additional Au (between 0.6 and 1.2 ML) on top of the c(2 × 2) surface alloy leads to dealloying, causing a segregation of the Au from the mixed c(2 × 2) layer to the overlayer. Supporting evidence for this assumption is that the intensities of the second shadowing peak as well as the blocking peak are decreased with increasing Θ_{Au}. At 1.2 ML coverage, the shadowing features at higher incidence angles due to scattering from the second- and third-layer Au atoms are totally eliminated, revealing that essentially no substrate Au is detected.

In order to determine the thermal stability of the Cu–Au surface alloys, LEIS signals were collected as a function of Au coverage at several different substrate temperatures. Figure 4 shows the Au/(Au + Cu) LEIS top-layer intensity ratio collected under double-alignment conditions at five different substrate temperatures. The results indicate that the intensity ratio exhibits a strong dependence on the substrate temperatures. For deposition even at 100 °C, extensive interdiffusion has already taken place, causing a decrease in the top-layer Au signals. A large change of the Au composition occurs at the substrate temperatures between 200 and 300 °C. Our measurements from the α-scans also indicate the formation of Cu_3Au-like surface alloy over three atomic layers (a typical coverage of 1 ML) in this temperature range (not shown). At 400 °C, a nearly pure Cu surface layer is formed on top of a dilute Cu–Au alloy. In addition, we also found that the alloy stoichiometry was identical when the Au was deposited onto a heated substrate, or deposited at RT and subsequently heated. This indicates that annealing increases the kinetics of alloy formation and allows the surface to come to equilibrium relatively rapidly.

3.2. Pd/Cu(001)

Direct evidence for a surface reconstruction during Pd deposition on Cu(001) at RT came from visual inspection of the LEED pattern. As shown in figure 5 above, the best c(2 × 2) structure is formed for $\Theta_{Pd} = 0.5$ ML. The p4g reconstruction is initiated for $\Theta_{Pd} \geqslant 0.6$ ML, becomes most prominent at 1 ML and falls off completely at 1.4 ML. The

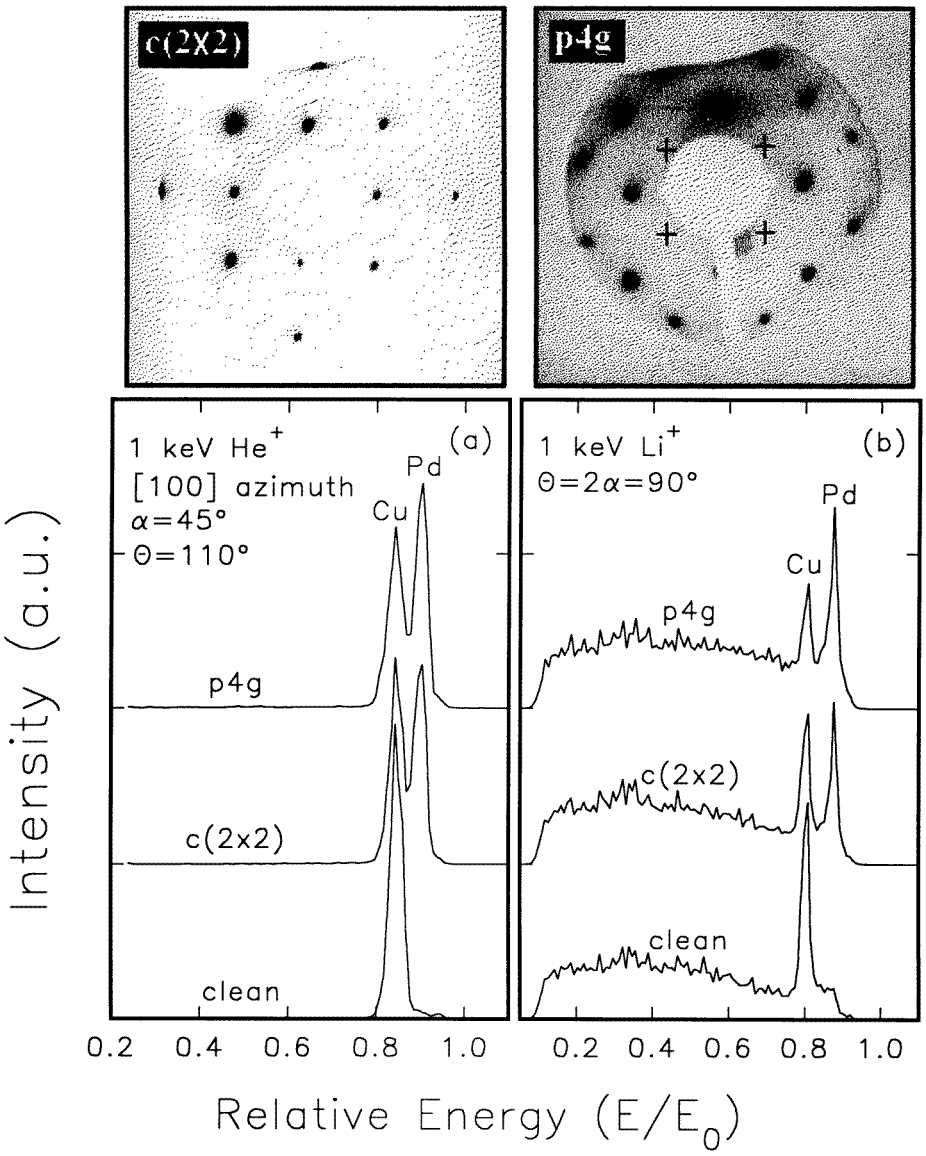

Figure 5. Typical energy spectra obtained from the clean Cu(001), c(2×2) (0.5 ML) and p4g (1 ML) surfaces using Li^+ ions ($\theta = 2\alpha = 90^\circ$) and He^+ ions ($\alpha = 45^\circ$ and $\theta = 110^\circ$) along the [100] azimuth. The top of the figure shows typical LEED patterns corresponding to Cu(001) c(2×2) at 78 eV (0.5 ML) and p4g at 51 eV (1 ML). The types of missing (0, 1/2) spots are marked by plus signs.

LEED pattern of the p4g reconstruction is in principle just a 2×2 pattern where every spot labelled $(0, n + 1/2)$ or $(n + 1/2, 0)$ is absent at normal incidence. Above 1.4 ML, a weak and diffuse (1×1) pattern with steaks along the [110] azimuth was observed.

Typical energy spectra of backscattered 1 keV He^+ and Li^+ ions from clean, c(2×2) and (2×2)p4g Cu(001) surfaces along the [100] azimuth at $\alpha = 45^\circ$ are shown in figure 5.

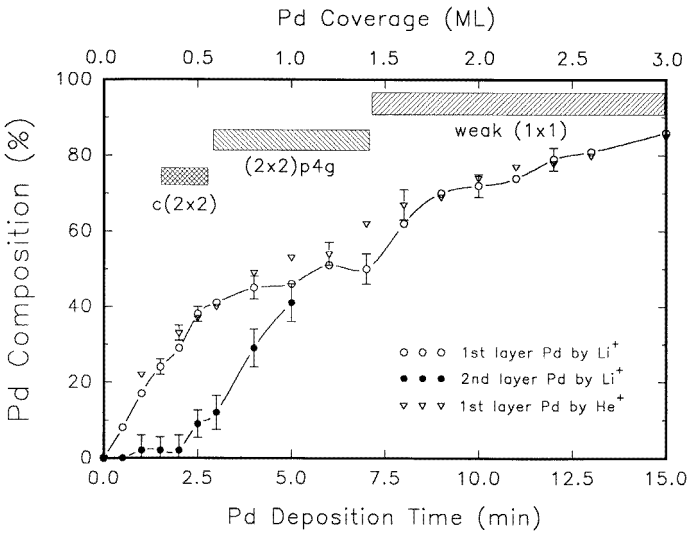

Figure 6. The Pd composition in the top two layers as a function of Pd deposition time. Error bars are based on 4–5 measurements.

In this geometrical scattering condition, the incident ions can only hit the first-layer atoms of a perfect fcc(001) face and the scattered ions from second and deeper layers are shadowed and/or blocked. A larger scattering angle of $\theta = 110^\circ$ was used for He^+ ions in order to improve separation of the scattered peaks from Cu and Pd atoms. As Pd is deposited, the Pd-peak intensity increases, while the Cu-peak intensity decreases. Two peaks appear near the values of E/E_0 expected from the binary collision model [16]: 0.90 for Pd and 0.84 for Cu at $\theta = 110^\circ$ in the He^+ spectra; 0.88 for Pd and 0.80 for Cu at $\theta = 90^\circ$ in the Li^+ spectra. An important feature of figure 5 is that the Pd signal in the top layer between the c(2×2) (0.5 ML) and the p4g (1 ML) structures is only slightly different, in contrast to the case for Au/Cu(001).

To give an idea of intermixing, a systematic study of Pd deposition as a function of coverage was performed. Using a simple shadow cone model analysis based on the fcc(001) geometry of atomic arrangements, we have determined the surface composition of the top two layers during Pd deposition. In this determination, the relative sensitivity factor and the degree of focusing were obtained using selective scattering geometries with standard measurements on pure Cu(001) and Pd(001) single crystals. To eliminate a number of systematic errors, we show in figure 6 the Pd composition as a function of Θ_{Pd} obtained using both Li^+ and He^+ ions; typical results are depicted for 1 keV. It is seen that the first-layer compositions obtained using Li^+ ions are consistent with the values derived for He^+ ions. At $\Theta_{Pd} = 0.5$ ML, the measured values for Li^+ ions for the c(2×2) structure show a Cu-rich surface (38% Pd) in the first layer, but there is a substantial Pd ($\sim$10%) content in the second layer, in good agreement with previous measurements carried out by several groups [10, 11, 15]. For the p4g phase at 1 ML Pd, the results show that there is 47% Pd in the first layer while the second layer has 42% Pd. LEIS data obtained from an incidence angle scan along the [310] azimuth indicate that about 10% Pd has diffused into the third and/or fourth layers [12].

In order to determine the ordering and symmetry of the mixed Cu–Pd surface, in figure

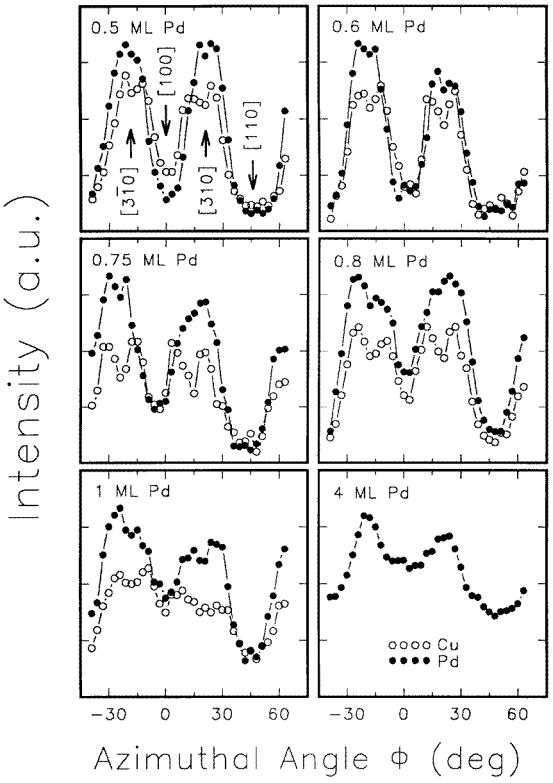

Figure 7. Azimuthal distributions of 1 keV Li^+ ions scattered from the Pd/Cu(001) surfaces at various Θ_{Pd} at $\alpha = 10^\circ$ and $\theta = 110^\circ$.

7 we show the Pd and Cu signals collected as functions of ϕ at different Θ_{Pd} at grazing incidence. Similarly to the c(2 × 2) Cu–Au case at 0.5 ML, for the c(2 × 2) structure the Cu and Pd ϕ-scans are identical in shape. This can only be true if the arriving Pd atoms are incorporated into the first layer by the replacing of surface Cu atoms, thus forming Cu adatoms. With further increasing Θ_{Pd}, the Cu and Pd intensities still show the same ϕ-dependence, but the main shadowing dips around $\phi = 0$ and 45° become less pronounced. For the p4g structure at 1 ML, we observe that a less ordered Cu–Pd surface layer is developed. These observations are indicative of atomic displacements and/or the onset of disorder at the surface. We believe that the observed less pronounced shadowing dips are made up of contributions from somewhat distorted surface domains, while disordered regions and domain boundaries increase the background intensity. This is consistent with the LEED observations showing the p4g symmetry with high background. At 4 ML, only Pd signals are detectable in the surface, revealing that a poorly ordered Pd(001) overlayer is formed.

Three observations, which relate to the structure of the p4g phase, have already been described. First, for local $\Theta_{Pd} \geqslant 0.6$ ML, the p4g reconstruction is initiated. On increasing Θ_{Pd} to 1 ML, the reconstruction becomes pronounced with two glide lines and hence systematic extinction of diffractions. Second, the p4g phase has two mixed Cu–Pd layers and it is necessary for an ordered c(2 × 2) precursor state to exist. Since the LEED experiments were conducted at low electron energies (∼50 eV), it was concluded that the

symmetry of the LEED pattern arose from a displacement of the top-layer atoms. Third, shadowing features observed from the ϕ-scans illustrate that the surface of the p4g phase is less ordered. Further experiments also revealed that the clock reconstruction was not observed on deposition of additional 0.5–0.7 ML of Cu onto the c(2×2) Cu–Pd layer (the formation of a pure Cu overlayer/c(2×2) Cu–Pd).

On the basis of the above considerations, two possible models for the p4g reconstructed surface can be proposed: (i) a pure Pd structure; and (ii) an ordered Cu–Pd layer. As the first model involves the pure Pd(001) overlayer wetting the underlying c(2×2) layer, this is not consistent with all of the results described above. Thus, a pure overlayer model can be excluded. One alternative model, which is still in the realms of speculation, proposes that the surface is an ordered c(2×2) Cu–Pd layer. However, this structure no longer belongs to the p4g space group because of the lack of mirror planes in the surface [22]. Instead, it becomes the lower-symmetry space group (2×2)pgg. Although the pgg symmetry still accounts for the spots missing from the LEED pattern, this ordered mixed Cu–Pd model seems unlikely because our LEED pattern shows broadened diffraction spots with high background and the angular scan shows the shallow dips along the main crystallographic directions. One possibility which can 'rescue' this model is that the Pd and Cu atoms may be randomly intermixed in the surface. Indeed, we found only the model of a randomly mixed Cu–Pd layer above an ordered c(2×2) layer to satisfy the constraints and to give a good representation of the LEED and LEIS measurements.

Accepting the model of a randomly mixed Cu–Pd layer, a question still remains as to whether the surface Pd atoms form any two-dimensional (2-D) islands. If so, a further question arises as to what is the lateral displacement (δ_{xy}) of the Pd atoms in the surface layer. These two questions can be addressed by measuring the ϕ-scans through K^+-ion scattering. The clustering effect of Pd atoms in the first layer can be examined by observing Pd–Pd pairs along the main azimuthal [110] direction using K^+ ions. K^+-ion scattering will exhibit a Pd–Pd double-scattering (DS) peak appearing at energies higher than the Pd single-scattering (SS) peak in the energy distributions if there is a Pd clustering, while a perfect ordered c(2×2)-like surface will result in pure Cu–Pd nearest neighbours along the [110] azimuth [20]. Figure 8 shows the DS intensity distributions over a range near the [110] azimuth taken from the Pd(001), Cu(001) and p4g surfaces with 2 keV K^+ ions at $\theta = 2\alpha = 90^\circ$. The K^+-ion scattering near the [100] azimuth was not carried out for analysis because the interatomic spacing along this direction is larger compared to that along the [110] azimuth, causing a weaker dependence of the DS peak intensities on the azimuthal direction.

A detailed analysis of the experimental angular distributions is made by comparison with the ϕ-scans calculated using our group's SABRE-93 code with 3-D simulation [23]. The SABRE code is based on a binary collision approximation in a manner similar to that used in the well known MARLOWE code [24]. The primary difference between MARLOWE and SABRE is that SABRE is dedicated to surface scattering simulation whereas MARLOWE can treat more general aspects of ion–solid interactions (see [23, 25] for details). In the following simulations, the structure used was constructed of three layers. For the p4g structure, the atoms of the ordered c(2×2) second layer and pure Cu third layer were at the positions of the ideal bulk Cu substrate. The ZBL potential was used in the simulations. The Debye temperatures used were 343 K for Cu and 270 K for Pd. For the clean Pd(001) and Cu(001) surfaces (figure 8(a)), the general feature obtained is that the DS peak intensity is very sensitive to the ϕ-direction near the [110] azimuth. The DS peak distributions in both surfaces exhibit full widths at half-maximum (FWHM) of their Gaussian distributions which are approximately equivalent to the instrumental broadening, suggestive of a single

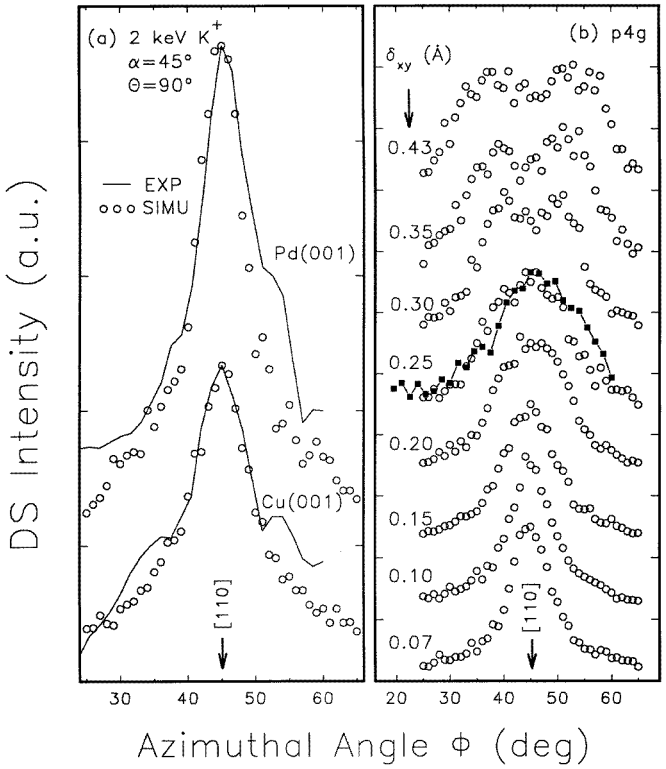

Figure 8. Experimental (dark squares with solid lines) and simulated (open circles) azimuthal distributions of 2 keV K^+ ions double scattered: (a) from Pd–Pd pairs in the clean Pd(001) surface and from Cu-Cu pairs in the Cu(001) surface; and (b) from Pd–Pd pairs for several different lateral displacements (δ_{xy}) in the p4g surface. The ion beam was incident at $\alpha = 45^\circ$ and $\theta = 90^\circ$. The experimental and simulated DS intensities have been normalized to the same height at $\phi = 45^\circ$.

fcc site in each case. Good agreement between the experimental data and the simulated curves is obvious. For the p4g structure in figure 8(b), we observe that the intensities of the Pd DS peak along the [110] azimuth are much weaker than those of the clean Pd(001) surface. We estimate that approximately ∼20% of the Pd atoms have Pd nearest neighbours in the surface layer by taking the ratio of the Pd DS intensity area between the p4g and simulated Pd overlayer surfaces. Thus, we suggest that the observed reconstruction is due to domains of a randomly mixed Cu–Pd region with some of pure Pd islands above the underlying c(2×2) layer.

The most important structural information in figure 8(b) is that for the 1 ML p4g phase the ϕ-distribution (dark squares with solid lines) is very broadened near the [110] azimuth and the FWHM is ∼6–7° wider compared to the ϕ-distribution of the Pd DS intensity in either the clean Pd(001) surface or the Cu(001) surface. The broadening in the DS intensity implies a less ordered surface layer, mediated through a surface clock reconstruction. By comparison to the simulation results for several different values of the lateral displacement of the Pd atoms, the best match of the data to a model simulation, having the same FWHM in the angular distributions, is obtained for a value of the lateral clockwise–anticlockwise

displacement of the Pd atoms parallel to the surface to be 0.25 ± 0.07 Å, in good agreement with the recent value of 0.28 Å [15]. This corresponds to the rotation angle of $8 \pm 2^{\circ}$.

The present p4g structure on Cu(001) is only a metastable phase. Further experiments reveal that annealing to 230 °C for several minutes leads to a gradual transition to the c(2×2) structure. The LEIS measurements indicate that the second-layer Pd atoms have diffused into the deeper layers and only the ordered c(2 × 2) surface alloy exists at the surface. This indicates that only the Cu_3Pd phase is thermodynamically stable on the Cu(001) surface.

4. Discussion

A thermodynamical criterion based upon the surface energies of the substrate (γ_s) and film overlayers (γ_f) and upon the interfacial energy (γ_{int}) has been traditionally established for predicting the growth mode [26]. If the system minimizes the surface free energy, then for $\Delta\gamma = \gamma_f + \gamma_{int} - \gamma_s < 0$ layer-by-layer (Frank–van der Merwe) growth is expected, while for $\Delta\gamma \geqslant 0$, three-dimensional (3D) (Volmer–Weber) growth is expected. It has been argued that in highly strained systems with $\Delta\gamma < 0$, the Stranski–Krastanov growth mode should also be predicted (with completion of the first layer followed by 3D growth in subsequent layers). According to this rule, the large negative surface energy difference between gold (0.34 eV/atom [27]) and copper (0.47 eV/atom [27]) should favour layer-by-layer growth for Au on Cu(001), while the large positive surface energy difference between palladium (0.54 eV/atom [27]) and copper should favour a 3D cluster growth for Pd on Cu(001). Indeed, these two different growth models were observed at low temperatures (below −50 °C for Au/Cu(001) [1] and below −173 °C for Pd/Cu(001) [13]). At higher temperatures, however, the Au and Pd growth mechanisms on Cu(001) are different.

From a thermodynamical point of view, the system tends to form the energetically most favourable configuration, while kinetics determines the growth behaviour of the film. Due to the existence of a kinetic pathway for intermixing, Au is incorporated in the Cu(001) surface at RT, forming a c(2 × 2) surface at $\Theta_{Au} = 0.5$ ML. We have shown that the mixed c(2 × 2) Cu–Au surface alloy in the top layer has a measurable amount of second- and/or third-layer Au atoms present, even if the Au segregation towards the surface is energetically favoured. A considerable roughing of the surface during deposition may account for Au atoms being buried deeply. As the Θ_{Au} increases from 0.6 ML to about 1.2 ML, dealloying occurs. This is evident from the simultaneous complete loss of the c(2 × 2) LEED pattern and development of a hcp LEED pattern. At 1.2 ML, we no longer see any traces of Au penetrating into the Cu substrate in the LEIS angular scans. The elimination of the surface alloy and the formation of a nearly pure Au overlayer support this dealloying model. The driving force for the dealloying and island formation is the strong surface segregation of Au in Cu. This can be obviously ascribed to two causes: first, Au has a surface energy/atom smaller than that of Cu by 0.13 eV [27]; and second, the Au atom is 15% larger than Cu. Both effects favour Au segregation.

From ion scattering the surface buckling of the Cu and Au atoms in the Cu–Au surface was measured to be $D_0 = 0.12 \pm 0.06$ Å. This determination (once potential calibrated) of the surface vertical buckling is direct, and independent of the first and second interlayer spacings and possible relaxation in the second or deeper layers. An advantage of low-energy alkali-ion scattering is that, unlike electron and atom diffraction, it provides mass-selective real-space information on the atomic arrangement at the surface without requiring sophisticated model calculations.

For the Pd on Cu(001) case, the RT reaction also leads to the formation of an ordered surface alloy due to the intermixing of Pd with Cu. After deposition of 0.5 ML Pd, the

first c(2 × 2) surface alloy is completed. From considerations of surface energy, Pd atoms landing on the Cu(001) surface are incorporated into the surface, therefore gaining energy through three related effects:

(i) by reducing the number of unsaturated bonds compared to undercoordinated Pd atoms sitting on the surface;
(ii) by maximizing the number of Cu–Pd bonds; and
(iii) by lowering the surface free energy to increase Cu atoms in the top layer.

These considerations of lowering surface free energy would favour a Cu-rich surface, in good agreement with our LEIS measurements. After increasing Θ_{Pd} to 0.6 ML, the incorporation of further Pd atoms into the Cu adatoms leads to the Cu–Pd surface alloy in the top layer. Since not all Pd atoms can overcome the energetic barrier to replace surface Cu adatoms and thereby form a second surface alloy layer, some regions with Pd islands may be formed. Thus, we conclude that a certain critical Θ_{Pd} has to be established above the underlying c(2 × 2) layer before the reconstruction is initiated. At 1 ML, a second surface alloy containing some of the Pd islands with a p4g reconstruction is formed, in good agreement with the experimental observations.

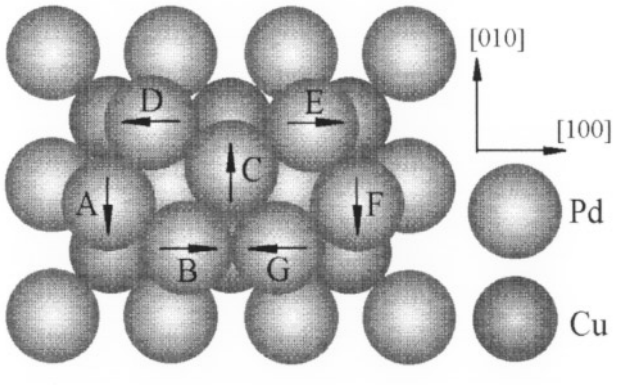

Figure 9. A hard-sphere model for the p4g structural model: the lateral clockwise–anticlockwise displacement of the surface Pd atoms above the ordered c(2 × 2) Cu–Pd layer. A randomly intermixed Cu–Pd region above a c(2 × 2) Cu–Pd layer (no contribution to the p4g symmetry) is not shown.

On the basis of the experimental results and proposed model, the driving force for the reconstruction must therefore be directly related to the interaction between surface Pd islands and the underlying c(2 × 2) layer. It is conceivable that the clock reconstruction is formed by Pd covering islands of the underlying c(2 × 2) layer. In the top two layers, the Pd atoms are under considerable compressive stress due to the 7.8% lattice mismatch between Pd and Cu. The stressed underlying c(2 × 2) layer relaxes at the boundary and exerts a force on the top layer. To relieve surface stress, neighbouring compressed Pd atoms in the top layer share in a collective way the cost of inducing a p4g clock reconstruction in which the squares of Pd atoms surrounding the underlying Pd atoms rotate laterally. Energetically, this is the 'cheapest' way to lower the surface island energy. This strain-relief mechanism clearly demonstrates that the roughness of the underlying mixed layer introduced by the size difference provides a novel driving force for the lateral displacement of the upper-layer atoms. From a hard-sphere model, the driving mechanism for the reconstruction can be

understood. Because of the size difference between Pd and Cu in the underlying c(2×2) layer, the equilibrium position (only two possible sites) for the upper-layer atom is then shifted to the hollow site somewhere between two Pd and one Cu atoms as shown in figure 9. If the atom A in the surface layer displaces down to the equilibrium hollow site, as a consequence, the atoms B, C and D can only move right, up and left respectively to get to the equilibrium sites. In the same way the atoms E, F and G can only move right, down and left respectively to reach their equilibrium sites because of the direction of movement of the atom C. Detailed theoretical calculations are needed to explain why it is energetically most favourable to relieve the stress via a lateral displacement of the surface Pd atoms.

5. Conclusion

The structure and growth of ultrathin Au and Pd films on Cu(001) at RT have been studied using LEIS in combination with LEED. We have demonstrated that the mixed c(2×2) surface alloy of nominally 0.5 ML Au/Cu(001) has a measurable amount of second- and third-layer Au atoms present. Between 0.6 and 1.2 ML, dealloying takes place, leading to a segregation of the Au from the underlying c(2×2) layer to the surface. For Pd on Cu(001), we have presented the first evidence for a surface reconstruction induced by a subsurface mixed c(2×2) layer. This produces the glide planes and leads to the experimentally observed systematic extinction of $(0, n + 1/2)$ and $(n + 1/2, 0)$ LEED spots at normal incidence. In good agreement with a recent study, the lateral clockwise–anticlockwise displacement is determined to be 0.25 Å. The reconstructing of the surface to relieve the stress by driving the clock rotation appears to be a more general phenomenon. The results may have general implications for the interaction of metal atoms of different sizes.

Acknowledgment

The authors gratefully acknowledge the financial support of this work by the Australian Research Grants Scheme.

References

[1] Palmberg P W and Rhodin T N 1968 *J. Appl. Phys.* **39** 2425
[2] Wang Z Q, Li Y S, Lok C K C, Quinn J, Jona R and Marcus P M 1987 *Solid State Commun.* **62** 181
[3] Graham G W 1987 *Surf. Sci.* **184** 137
[4] Hansen J C, Wagner M K and Tobin J G 1989 *Solid State Commun.* **72** 319
[5] Naumovic D, Stuck A, Greber T, Osterwalder J and Schlapbach L 1992 *Surf. Sci.* **269/270** 719
[6] Hansen J C, Benson J A, Clendening W D, McEllistrem M T and Tobin J G 1987 *Phys. Rev.* B **36** 6186
[7] Naumovic D, Aebi P, Stuck A, Schwaller P, Osterwalder J and Schlapbach L 1994 *Surf. Sci.* **307–309** 483
[8] Nakanishi S, Kawamoto K and Umezawa K 1993 *Surf. Sci.* **287/288** 974
[9] Wu S C, Lu S H, Wang Z Q, Lok C R C, Quinn J, Li Y S, Tian D, Jona F and Marcus P M 1988 *Phys. Rev.* B **38** 5363
[10] Graham G W 1986 *Surf. Sci.* **171** L432
[11] Graham G W, Schmitz P J and Thiel P A 1990 *Phys. Rev.* B **41** 3353
[12] Yao J, Shen Y G, O'Connor D J and King B V 1995 *J. Vac. Sci. Technol.* A **13** 1443
[13] Pope T D, Anderson G W, Griffiths K, Norton P R and Graham G W 1991 *Phys. Rev.* B **44** 11 518
[14] Anderson G W, Jensen K O, Pope T D, Griffiths K, Norton P R and Schultz P J 1992 *Phys. Rev.* B **46** 12 880
[15] Pope T D, Vos M, Tang H T, Griffiths K, Mitchel I V, Norton P R, Liu W, Li Y S, Mitchell K A R, Tian Z J and Black J E 1995 *Surf. Sci.* **337** 79
[16] Niehus H, Heiland W and Taglauer E 1993 *Surf. Sci. Rep.* **17** 213
[17] Detzel T, Memmel N and Fauster T 1993 *Surf. Sci.* **293** 227

[18] Overbury S H, Mullins D R, Paffett M T and Koel B E 1991 *Surf. Sci.* **254** 45
[19] Shen Y G, O'Connor D J and MacDonald R J 1992 *Surf. Interface Anal.* **18** 729
[20] Shen Y G, O'Connor D J, Wandelt K and MacDonald R J 1995 *Surf. Sci.* **328** 21
[21] The calibration of Li–Cu and Li–Au potentials was obtained from the measurements of the critical angle α_c as a function of scattering angle θ along one given azimuth on the clean $Cu_3Au(001)$ surface.
[22] Onuferko J H, Woodruff D P and Holland B W 1979 *Surf. Sci.* **87** 357
[23] O'Connor D J 1978 *PhD Thesis* Australian National University
[24] Robinson M T and Torrens I M 1974 *Phys. Rev.* B **9** 5008
[25] Danailov P M, O'Connor D J and Snowdon K J 1996 *Surf. Sci.* **347** 215
[26] Bauer E and van der Merwe J H 1986 *Phys. Rev.* B **33** 3657
[27] Chang T M and Carter E A 1994 *Surf. Sci.* **318** 187